# Reservoir effect and the role of low current density regions on electromigration lifetimes in copper interconnects

Shao, W.; Chen, Z.; Tu, K. N.; Gusak, A. M.; Gan, Zhenghao; Mhaisalkar, Subodh Gautam; Li, Hong Yu

2006

Gan, Z., Shao, W., Mhaisalkar, S. G., Chen, Z., Li, H., Tu, K. N., et. al. (2006). Reservoir effect and the role of low current density regions on electromigration lifetimes in copper interconnects. Journal of materials research, 21(9), 2241-2245.

https://hdl.handle.net/10356/94915

https://doi.org/10.1557/JMR.2006.0270

---

# Reservoir effect and the role of low current density regions on electromigration lifetimes in copper interconnects

Z.H. Gan,[a] W. Shao, S.G. Mhaisalkar, and Z. Chen
*School of Materials Science and Engineering, Nanyang Technological University, Singapore 639798*
Hongyu Li
*Institute of Microelectronics, Singapore 117685*
K.N. Tu
*Department of Materials Science and Engineering, University of California—Los Angeles, Los Angeles, California 90095-1595*
A.M. Gusak
*Cherkasy National University, Cherkasy 18017, Ukraine*

(Received 19 February 2006; accepted 18 April 2006)

Electromigration (EM) in copper dual-damascene interconnects with extensions (also described as overhang regions or reservoirs) in the upper metal (M2) were investigated. It was found that as the extension length increases from 0 to 60 nm, the median-time-to-failure increased from 50 to 140 h, representing a ~200% improvement in lifetimes. However, further increment of the extension length from 60 to 120 nm did not result in any significant improvement in EM lifetimes. Based on calculations of current densities in the reservoir regions and recently reported nucleation, void movement, and agglomeration-based EM phenomena, it is proposed that there is a critical extension length beyond which increasing extension lengths will not lead to longer EM lifetimes.

## I. INTRODUCTION

It is well known that the interfacial diffusion at Cu/$Si_3N_4$ interfaces adversely affects the electromigration (EM) lifetime in Cu interconnects, in contrast to grain-boundary diffusion in Al alloy conductors.[1,2] Considerable attention has been paid to modify this interface to improve EM lifetime. Some researchers have used different cap materials,[3–5] and others have proposed different process treatments prior to the deposition of the dielectric cap.[6] Another good choice for delaying the EM failure is to introduce an extension (also described as overhang region or reservoir) in the interconnects.[7] It is thought that the extension serves as a reservoir for void growth, thus prolonging the median time to failure. Recently, the reservoir effect in Al–Cu interconnect with W vias was reported,[8,9] where voids are generally initiated at the W/Al interface by large Al atomic flux divergence. Lower levels of stress and vacancy concentration in the longer reservoir were proposed to contribute to the better electromigration reliability of interconnects. However, the reservoir mechanism in dual-damascene Cu interconnects is clearly different from that of W/Al via structures because voids nucleate at the Cu/$Si_3N_4$ interface far from the cathode and move along the interface.[10] Because of the technological importance of dual-damascene Cu interconnects, it is necessary to understand how extension lengths impact electromigration lifetimes. In this work, the reservoir effect and the role of low current density regions on electromigration lifetimes in Cu dual-damascene interconnects were investigated.

## II. EXPERIMENTAL

Test structures consisting of M1 and M2 via-fed structures (Fig. 1) were fabricated using 0.18 μm Cu/oxide damascene technology. M2 trench and via were formed by a via-first dual damascene process. Formation of M2 Cu metallization in undoped silicate glass (USG) trenches involved deposition of a stack of 25-nm Ta barrier, 150-nm physical vapor deposited (PVD) Cu seed, and 600-nm electrochemical plated (ECP) Cu layers. A cap of 50 nm $Si_3N_4$ was deposited after Cu chemical mechanical polishing (CMP) process. Layers of 800-nm USG, 50-nm $Si_3N_4$, and 500-nm USG were then deposited as intermetal dielectric. A 50-nm-thick $Si_3N_4$ served as the trench 2 etch-stop layer. M2 was 350 nm thick and

---

[a] Address all correspondence to this author.
e-mail: EZHgan@yahoo.com.sg

DOI: 10.1557/JMR.2006.0270

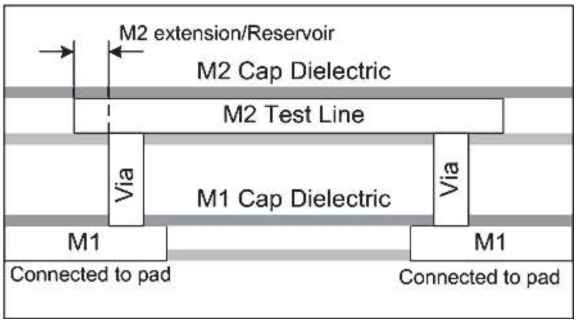

FIG. 1. Schematic cross section of M2-via test structure.

via diameter was 260 nm. The M1 lines connected to pads were short and wide such that voids would be formed in the narrow and long M2 test line between the vias. The M2 test lines were 500 μm long and 280 nm wide.

EM tests were performed in a *Qualitau* (QualiTau, Inc., Santa Clara, CA) package level EM test system. To study the reservoir length effect on EM, M2 structures with extensions of 0, 60, and 120 nm were tested at 300 °C with a current density of 1.2 MA/cm$^2$. In each case, 12 samples were tested. Focused ion beam (FIB) and transmission electron microscopy (TEM) were used for post-EM failure analysis.

## III. RESULTS AND DISCUSSION

The cumulative distribution of failure time for three different extensions of M2 test structures are shown in Fig. 2. The distributions could be described well with log-normal distributions with similar slopes, thus indicating similar failure modes in these structures. As the M2 extension was increased from 0 to 120 nm, the EM lifetime was improved correspondingly. For samples without extension, Mean-time-to-failure (MTTF) was about 50 h, whereas it was about 140 h (i.e., close to a 200% increment) in the case of 60-nm extension. However, as the extension length was further increased from 60 to 120 nm, EM lifetimes did not show significant further improvement.

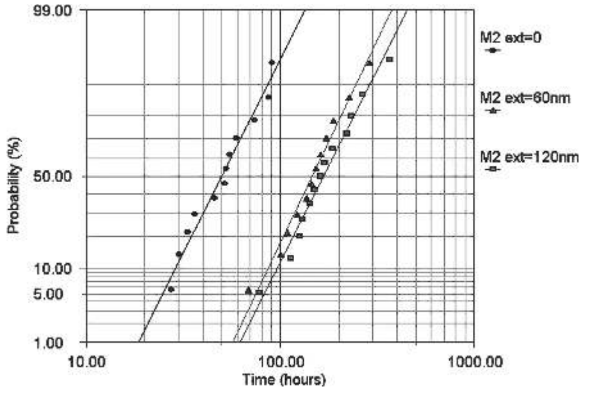

FIG. 2. Cumulative Distribution Function (CDF) plot of median-time-to-failure for 280-nm-wide M2 copper lines with three different M2 extensions.

A post-EM cross-sectional FIB image of a 120-nm-extension with 10% resistance increase is shown in Fig. 3(a). It is clearly seen that at the initial stage of EM, void nucleation takes place preferentially at the Cu/Si$_3$N$_4$ interface in the M2 line away from the cathode via. It is interesting to note that in departure from the current understanding of the EM mechanism based on tensile stress-based void nucleation[11] and current density gradient induced void diffusion,[7] the corner of the M2 line above the via is free from voiding. Because of the stress-induced void nucleation mechanism, voids would be expected to nucleate at the cathode end of the via as well as at the via bottom during EM, where high tensile stress develops due to the blocking boundary formed by the Ta liner. When the critical tensile stress for void nucleation is reached, voids may form and grow, leading to via opening.[12] It is also evident that the current crowding-induced vacancy flux mechanism[7] does not apply either to the observed failure mode [Fig. 3(a)]. This current crowding-based mechanism postulates that a current density gradient force drives vacancies from high current density to low current density regions. Accordingly, voids would nucleate at the top corner of the cathode end in the M2 interconnect.

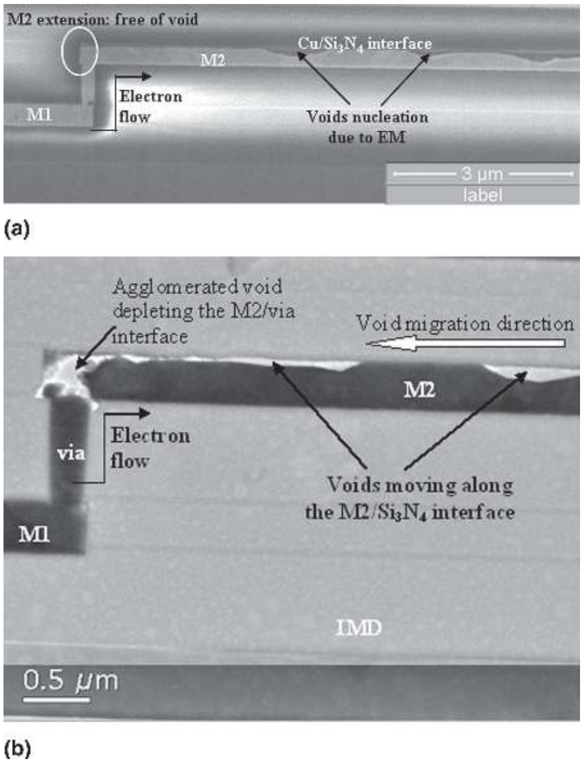

FIG. 3. (a) Cross-sectional FIB image induced by electromigration after 10% resistance increase, and (b) cross-sectional TEM image after 30% resistance increase.

At the 30% failure criterion for a 120-nm extension structure, the cross-sectional TEM image [Fig. 3(b)] shows that the EM-induced void has moved/grown along the Cu/dielectric-cap interface of the M2 trench against the electron flow direction, mainly driven by the electron wind force.[10] These observations lend further support to the hypothesis that voids form heterogeneously at the Cu/$Si_3N_4$ interface away from the cathode, migrate via interfacial diffusion paths at this interface driven by the electron wind force, accumulate near the cathode, and eventually lead to opening of the via and open circuit failure.

The localized current density at the via/M2 extension region was evaluated by finite element analysis (FEA). Figure 4 shows the contours of current density (solid curves) around the M2 extension/via region for three extension lengths. The contours of current density gradient (dotted curves) have been overlayed on the current density contours. After the interfacial void is generated in the middle section of the metal strip away from the via [Fig. 3(a)], where the current is uniform and parallel to the interface, the void migration along current direction is driven by the electron wind force (i.e., $F_c$):

$$F_c = -Z^*e\rho j \quad , \tag{1}$$

where $Z^*$ is the effective charge number of the diffusing Cu atom, ρ is the resistivity of Cu, and $j$ is the current density. The void velocity $v$ is related to the current density by the following equation[13]:

$$v = -(3ND_s\Omega/kTa)A\ Z^*e\rho j \quad , \tag{2}$$

where $N$ is atomic density, Ω is the atomic volume, k is the Boltzmann constant, $T$ is the temperature in Kelvin, $a$ is the radius of the void, $D$ is the diffusion constant, and $A$ is a factor related to the void location.

Another driving force due to current-density gradient (i.e., $F_g$)[7] may also influence the void migration

$$F_g = -\mathrm{d}P/\mathrm{d}\mathbf{r} \quad , \tag{3}$$

where $\mathbf{r}$ is the three-dimension vector, $P$ $(= q_v|j|A\Delta R_v)$ is the potential energy of an excess vacancy driven by the current density $j$, $q_v$ is the charge of the vacancy, $A$ is the scattering cross section of the vacancy, and $\Delta R_v$ is the resistance of the excess vacancy.

However, analyzing Eqs. (1) and (3) using the material parameters[14–16] $q_v = Z^*e = 4e$, $A = 1 \times 10^{-15}$ cm$^2$, $\Delta R_v = 1 \times 10^4\ \Omega$, and $\rho = 1.67 \times 10^{-6}\ \Omega$ cm leads to the inference that $F_g$ is at least one order of magnitude lower than $F_c$ for the location along the M2/$Si_3N_4$ interface as well as at the current density contours (e.g., 0.4 MA/ cm$^2$), where the values of $|\mathrm{d}j/\mathrm{d}\mathbf{r}|$ are between $2 \times 10^{10}$ and $3 \times 10^{10}$ A/cm$^3$. Therefore, the effect of current density gradient ($F_g$) could be ignored in the present study.

We propose that there exists a low current density region (dead-zone) bounded by a critical low current density ($j_{crit}$) around the upper-left corner [Fig. 5(a)] that highly retards the movement of the incoming voids and may prevent or resist void entry into the M2 extension. Figure 5(a), derived from Fig. 4, presents current density contours of $j = 0.4$ MA/cm$^2$ for extensions of 0 to 120 nm. It should be noted that the current density contours for different extensions have been overlayed along with the M2/via geometry to provide a direct comparison of the change in contours as a function of extension lengths.

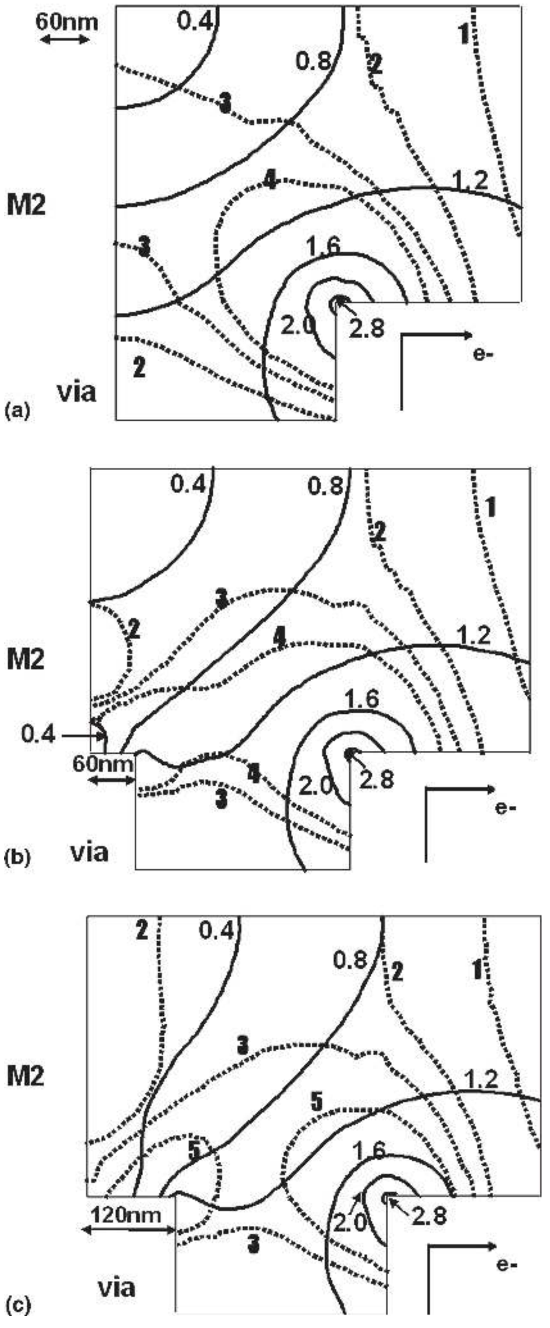

FIG. 4. Contours of current density (solid curves, unit: MA/cm$^2$) around the M2 extension/via region for (a) 0-extension, (b) 60-nm extension, and (c) 120-nm extension. The contours of gradient of current density (dotted curves, unit: $10^{10}$A/cm$^3$) in M2 are overlapped.

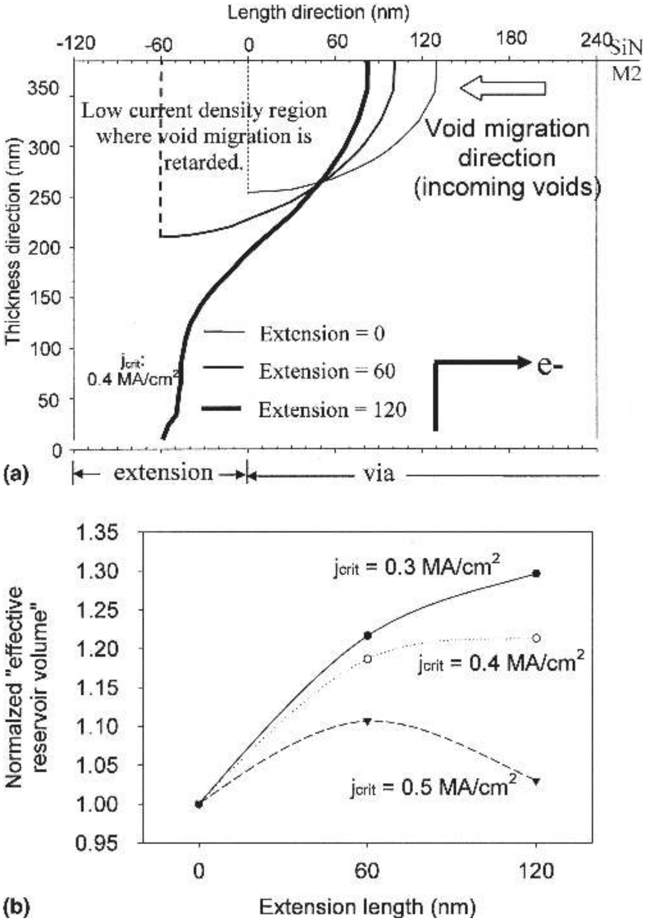

FIG. 5. (a) Overlapped contour lines around the extension region corresponding to 0.4 MA/cm$^2$ for varied M2 extensions, indicating a low current density zone that may retard further movement of incoming voids. (b) Normalized "effective reservoir volume" in terms of extension length.

It may be envisaged that the incoming voids are retarded near a $j_{crit}$ boundary, slowing down or even perhaps blocking their progress into the low current density regions located at the far corners of the reservoirs. Only a part of the extension volume may effectively serve as a reservoir for accumulation.

It is observed in Fig. 5(a) that the low current density zone changes shape and shifts slightly to the left with varying M2 extensions. It is thus instructive to compare the "effective reservoir volume" above the via/M2 interface, which is defined here as the low current density volume was subtracted from the overall geometrical volume. We use the effective reservoir volume of 0 extension as an internal standard to normalize all three cases with varied extension length. The normalized effective reservoir volumes for current densities of 0.3–0.5 MA/cm$^2$ are plotted with respect to the extension length in Fig. 5(b). It is seen that for 0 and 60 nm M2 extensions, the effective volume serving as void accumulation reservoir increases with increasing extension lengths at all current densities. However, this trend may change for the 120 nm extension [Fig. 5(b)] because of current crowding around the via region evident in Fig. 4. It may thus be summarized that increasing extension length from 0 to 60 nm increases effective reservoir volume, thus increasing the void volume that leads to via opening and improved EM lifetimes. However, further increase in M2 extension to 120 nm does not increase this effective reservoir volume and does not significantly improve EM lifetimes any further. This concept of effective reservoir volume successfully explains the experimental observations that MTTF was doubled with extension increase from 0 to 60 nm whereas there was arguably a ~5–10% enhancement on MTTF as the extension length was further increased from 60 to 120 nm. The data analysis thus indicates that 60 nm may be the critical extension length beyond which increasing extension sizes have no effect on EM lifetimes. The effective reservoir volume plot [Fig. 5(b)] also suggests that the critical current density, below which significant void migration does not take place, may be on the order of 0.4 MA/cm$^2$.

## IV. CONCLUSIONS

In Cu dual-damascene interconnects, we propose that there is a low current density zone in the M2 extension corners above the cathode, which retards the void migration into the extensions. Accordingly, only part of the extension volume could serve as an effective reservoir for void accumulation. Based on the present analysis, a 60-nm extension appears to be the critical extension length, beyond which increasing extension sizes have no effect on EM lifetimes.

The implications of this retardation of void movement caused by low current density regions is wide ranging. Similar reservoirs (or reservoir like effects) are observed in interconnect tree structures[17] and in redundant double via structures.[11]

## REFERENCES

1. C.K. Hu, R. Rosenberg, and K.L. Lee: Electromigration path in Cu thin-film lines. *Appl. Phys. Lett.* **74,** 2945 (1999).
2. J.R. Lloyd and J.J. Clement: Electromigration in copper conductors. *Thin Solid Films* **262,** 135 (1995).
3. C.K. Hu, L. Gignac, R. Rosenberg, E. Liniger, J. Rubino, C. Sambucetti, A. Domenicucci, X. Chen, and A.K. Stamper: Reduced electromigration of Cu wires by surface coating. *Appl. Phys. Lett.* **81,** 1782 (2002).
4. C.K. Hu, L. Gignac, E. Liniger, B. Herbst, D.L. Rath, S.T. Chen, S. Kaldor, A. Simon, and W.T. Tseng: Comparison of Cu electromigration lifetime in Cu interconnects coated with various caps. *Appl. Phys. Lett.* **83,** 869 (2003).
5. Y. Shacham-Diamand and S. Lopatin: High aspect ratio quarter-micron electroless copper integrated technology: Invited lecture. *Microelectron. Eng.* **37–38,** 77 (1997).

6. A. von Glasow, A.H. Fischer, D. Bunel, G. Friese, A. Hausmann, O. Heitzsch, M. Hommel, J. Kriz, S. Penka, P. Raffin, C. Robin, H.P. Sperlich, F. Ungar, and A.E. Zitzelsberger: The influence of the SiN cap process on the electromigration and stressvoiding performance of dual damascene Cu interconnects in *Proc. 41st Annual Int. Rel. Phy. Symp.* (IEEE, Piscataway, NJ, 2003), p. 146.
7. K.N. Tu, C.C. Yeh, C.Y. Liu, and C. Chen: Effect of current crowding on vacancy diffusion and void formation in electromigration. *Appl. Phys. Lett.* **76,** 988 (2000).
8. Y.B. Park and I.S. Jeon: Effects of mechanical stress at no current stressed area on electromigration reliability of multilevel interconnects. *Microelectron. Eng.* **71,** 76 (2004).
9. I.S. Jeon and Y.B. Park: Analysis of the reservoir effect on electromigration reliability. *Microelectron. Reliab.* **44,** 917 (2004).
10. A.V. Vairagar, S.G. Mhaisalkar, A. Krishnamoorthy, K.N. Tu, A.M. Gusak, M.A. Meyer, and E. Zschech: In situ observation of electromigration-induced void migration in dual-damascene Cu interconnect structures. *Appl. Phys. Lett.* **85,** 2502 (2004).
11. C.L. Gan, C.V. Thompson, K.L. Pey, W.K. Chio, H.L. Tay, B. Yu, and M.K. Radhakrishnan: Effect of current direction on the lifetime of different levels of Cu dual-damascene metallization. *Appl. Phys. Lett.* **79,** 4592 (2001).
12. R.G. Filippi, G.A. Biery, and R.A. Wachnik: The electromigration short-length effect in Ti–AlCu–Ti metallization with tungsten studs. *J. Appl. Phys.* **78,** 3756 (1995).
13. P.S. Ho: Motion of inclusion induced by a direct current and a temperature gradient. *J. Appl. Phys.* **41,** 64 (1970).
14. V.P. Zhdanov: *Elementary Physicochemical Processes on Solid Surfaces,* (Plenum Press, New York, 1991), p. 52.
15. M.C. Gutzwiller: Dislocations and elections in metals, in *Atomic and Electronic Structure of Metals,* edited by J.J. Gilman and W.A. Tiller (ASM, Metals Park, OH, 1966), p. 231.
16. R.O. Simmons and R.W. Balluffi: Measurement of equilibrium concentrations of vacancies in copper. *Phys. Rev.* **129,** 1533 (1963).
17. A.V. Vairagar, S.G. Mhaisalkar, A. Krishnamoorthy, M.A. Meyer, E. Zschech, K.N. Tu, and A.M. Gusak: Direct evidence of electromigration failure mechanism in dual-damascene Cu interconnect tree structures. *Appl. Phys. Lett.* **87,** 081909 (2005).